Global Journal of Engineering and Technology Advances
eISSN: 2582-5003
Cross Ref DOI: 10.30574/gjeta
Journal homepage: https://gjeta.com/

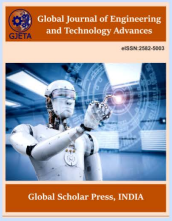

(RESEARCH ARTICLE)

Check for updates

# Study the effect of notches on bending fatigue strength of 2024 aluminum sheets

Hazim K Khalaf and Laith A Mahgoob *

*Department of Mechanical Engineering, College of Engineering, Tikrit University, Tikrit, Iraq.*

Global Journal of Engineering and Technology Advances, 2023, 14(01), 014–032

Publication history: Received on 23 November 2022; revised on 03 January 2023; accepted on 05 January 2023

Article DOI: https://doi.org/10.30574/gjeta.2023.14.1.0217

## Abstract

In the present study, the effect of holes on the curvature fatigue strength of 2024 aluminum sheets. Has been studied by taking a model of this type and cutting it into models with the dimensions required for testing and by using a central hole as the main variable by making a central whole (CH) with a diameter of (1mm). The device used in this research is a Reversed bending machine of type HI-TECH from a British origin, all tests were done at a constant stress ratio (R = -1), a rotational speed of 6000 rpm and a frequency (100 Hz). The study was practically and theoretically (using the ANSYS15.0 program). The results showed that stress is affected by the presence of holes and we notice increased stress in the samples that contain holes more than the core samples that do not contain holes and thus we notice that fatigue strength decreases in the samples that contain a central hole by (32%) of the core samples by the practical side on the theoretical side, strength of fatigue less than percentage (43.7%). The yield strength was found by tensile test equal to (73.6 MPa) and the ultimate tensile strength (195.2 MPa) as for the hardness value (59.7). Also, from the results obtained, it appears that streaking acts as stress centers, thereby increasing stress and thereby reducing the number of cycles and consequently failure.

**Keywords:** Aluminum alloy; Notch sensitivity; Strength reduction factor; Fatigue

## 1. Introduction

The cost resulting from sudden failures of various structures and mechanical parts, both economically and humanly, can sometimes be quite massive. Therefore, studies on total failure have taken a wide range of research and studies in the scientific and industrial fields. The emergence and progression of fatigue cracks in the wings and feathers of different aircraft leads to fatal failures. The onset of fatigue initiation or the onset of fatigue cracking appears as slippage on the face of the model and after a period of fatigue life becomes fixed and cannot be removed and with increasing number of cycles of loads, these slippage deepens and then cracks begin to form, and cracks in the stressful body can grow and progress in association The three phases. There is sufficient evidence that many engineering structures contain pre-established defects and these defects arise during plumbing or manufacturing, and therefore speculation begins with the beginning of fatigue and its growth from these defects in the metals used in the manufacture of hulls and aircraft vehicles. As the progression of fatigue cracking occurs very quickly, and for this reason, the onset of fatigue plays an important role in predicting the life of these compounds. And the growth of the fissure in a region where the region of the stress factor and low stress factor is very required because of this importance in determining the required age for these devices, therefore this region is the most controllable for determining the age range of fatigue that concerns aircraft. One of the basic requirements for any engineering structure is that it does not fail during Shelf life, so most of the engineer's skill is concentrated in realizing that there are several potential patterns of failure and in realizing how to prevent them [1]. The main patterns of mechanical failure that pertain to the designer as well as failure due to environmental corrosion can be listed as follows [2].

- (Elastic Buckling)

* Corresponding author: Laith A Mahgoob

- (Excessive elastic deformation)
- (Plastic deformation)
- (Creep)
- (Cracking)

The phenomenon of failure due to fatigue is described as the process of forming cracks, and its growth to an unstable measurement ends in sudden failure entirely due to the exposure of the parts to periodic periodic stresses, and the failure sometimes occurs with a change in the amount of load without a change in direction [3]. This failure is one of the most common types of failures in structures and mechanical parts [4،5].

The researchers studied (Qasim Bader, Emad Kadum, 2014) [6] the effect of the slitting (v) shape on the fatigue life in steel made from AISI 1037. Fatigue samples were made according to the specifications of the device used and made a (V) slit at different angles which are (30, 45, 90) degree and depth was (0.5, 2) mm. The study was practically and theoretically (using the ANSYS14.0 program), while the process was on a (Cantilever rotating-bending fatigue testing) at room temperature and frequency (50 Hz) and (R = -1), in this work the age of fatigue was verified The bending of the notched samples and thus the mathematical form of the formula for the fatigue life of samples was obtained. Note that in most cases it was found that the expected fatigue life was lower compared to the experimental values for all types of notched samples, this may be due to the fact that the fatigue life was predicted on the basis of the greatest stress in the notched section.

The researcher (D. W. Draket, 2015) [7] studied the effect of streaking and fatigue resistance, and many types of internal and external streaks have been studied in various forms. The factors controlling the slitting resistance were discussed, either from constant resistance or fatigue resistance, and it was found that the increase in the yield rate will usually increase the fixed efficiency of the slitting samples, but this increase may be limited by the ability of the material to react. It has been suggested that the use of high-resistance aluminum alloys in aircraft structures may produce a significant reduction in the structural weight of the same fixed resistance, but this may be accompanied by a decrease in fatigue resistance to the structures.

The researcher (Shaima Abdul Khader Hamza, 2018) [8] studied the effect of fixed and variable capacitance loads on the fatigue life of a low carbon steel alloy, the sample dimensions are of a length of (88.9 mm) and a width (30.1625 mm) and peripherally shortened from the middle, Fixed and variable capacity fatigue tests were performed using an Avery 7305 type device which operates by a 1420 rpm reverse-curving method. The higher the projected stress, the fewer cycles needed to fail, that is, the less fatigue life. In the case of fixed loads, fatigue life is greater compared to variable loads, where the number of turns required for failure is greater, and therefore the time required to form and grow the incision is greater.

The researchers studied (J. M. G. Martinez, et.al., 2019) [9] the effect of the size of the geometry on the prediction of the fatigue life of aluminum holes with small holes using critical distance methods. The wires used in the study are made of aluminum alloy 6201-T81. Servo-hydraulic testing machines were used with frequency (20 Hz) and (R = -1). Surround and V-Notch grooves, circular and many types of grooves were used. This research has been studied in theory (using FEM) and in practice. The LM obtained the best results by looking at all the small holes together, all expectations showed good adherence in this way with (84% for TH and (92%) for BH. The results of prediction of fatigue life in the small holes using the TCD method were satisfactory.

On this paper, the study of Notches and their effect on the resistance of the curvature of fatigue to aluminum sheets 2024, in practice and theory, using the program (ANSYS-Workbench) and by shedding the alternating stress of fatigue samples at a stress ratio (R = -1).

## 2. Experimental Work

### 2.1. Material Selection

Aluminum alloy (2024-O) with a thickness of (2.5 mm) is used in this study. It is one of the second series alloys with the basic alloy elements (Al. Cu. Mg). The main properties of this series are heat treatment and high strength at room temperature and also in degrees of High temperature. The Table (1) Chemical composition of aluminum alloy (AA2024) and its comparison with standard composition and Table (2) Real and standard mechanical, physical, and aluminum alloy properties (AA2024).

**Table 1** Chemical composition of aluminum alloy (AA2024) and its comparison with standard composition [10]

| Element (wt %) / Material | Si | Fe | Cu | Mn | Mg | Cr | Zn | Ti | Al |
|---|---|---|---|---|---|---|---|---|---|
| Standard | 0.5Max | 0.50 Max | 3.8-4.9 | 0.3-0.9 | 1.2-1.8 | 0.1 | 0.25 Max | 0.15Max | Bal. |
| Measured | 0.131 | 0.260 | 4.49 | 0.61 | 1.32 | 0.006 | 0.04 | 0.08 | Bal. |

**Table 2** Real and standard mechanical, physical, and aluminum alloy properties (AA2024) [10]

| | Tensile Yield strength ($\sigma_y$) (MPa) | Ultimate Tensile strength ($\sigma_u$) (MPa) | Elongation (El %) | Hardness Vickers (HV) | Modulus of Elasticity (GPa) |
|---|---|---|---|---|---|
| Standard Value | 75 | 185 | 20 | 47 | 69 |
| Actual Value | 73.6 | 195.2 | 18.8 | 59.7 | ---- |

### 2.2. Tensile Test

Samples of the tension test were manufactured using (Water Jet) device, according to the dimensions specified according to the international standard [ASTMB557M] for the aluminum samples as shown in Figure (1). The test was carried out on a computer-equipped (SANS-Universal Testing Machine) tensile testing device located at Mosul University / Mechanical Engineering Department laboratories as shown in Figure (2), and it is an automated device with a capacity of (100) tons to shed a slowly increasing tension load (Monotonic Load) on the samples, and the examination was conducted at a displacement control rate of (0.3mm / min) until failure occurred. I calculated engineering stress and strain using the following relationships [11].

$$\sigma = \frac{F}{A_o} \ldots\ldots\ldots\ldots\ldots\ldots \quad (1)$$

$$\varepsilon = \frac{\Delta L}{L} \ldots\ldots\ldots\ldots\ldots\ldots \quad (2)$$

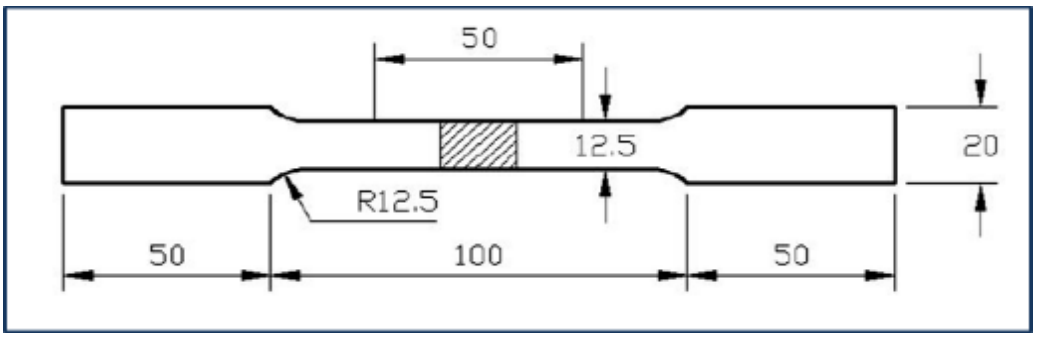


**Figure 1** Standard Dimensions of Tensile Test Samples According to the International Standard (ASTM B557M) (All Dimensions in Millimeters) [12]

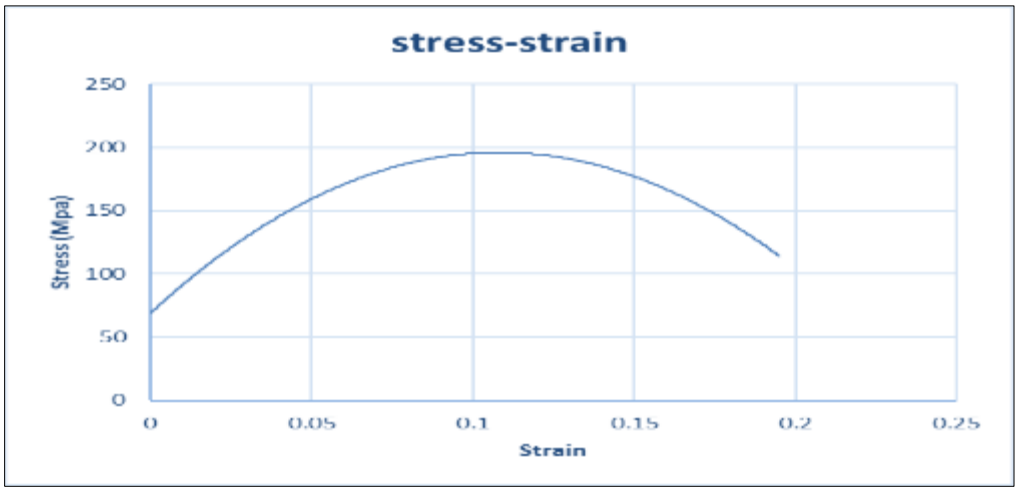


**Figure 2** Curve Stress and Strain of Aluminum Alloy (2024)

### 2.3. Fatigue Test

The device used in this research is the Reversed bending machine (HI-TECH) of British origin as shown in Figure (3). All tests were performed at a value of R = -1. The test sample is exposed to a load projected from the left side of the sample gasket perpendicular to the axis of the sample designated for the test. Thus, the sample segment is subjected to the curvature stress and by continuously this opposite curvature with the same value up and down leads to fatigue failure and fracture of the sample. The device is equipped with a meter to record the number of stress cycles. All tests were conducted at a rotational speed of 6000 rpm and a frequency of 60 Hertz.

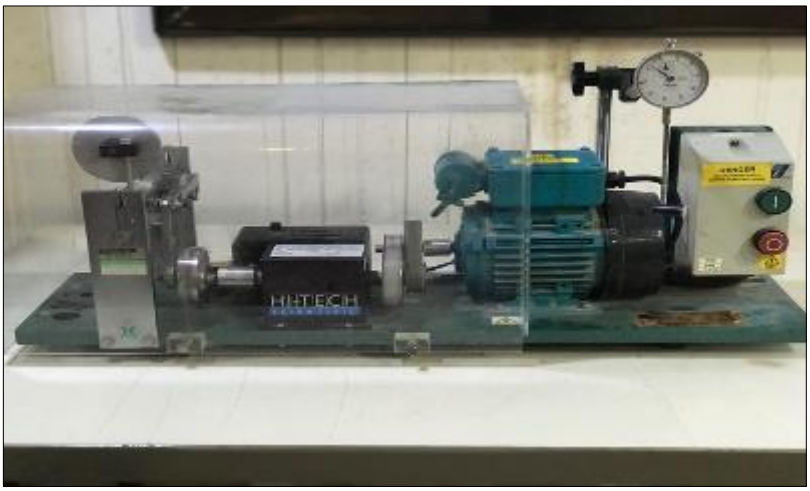


**Figure 3** Fatigue test machine

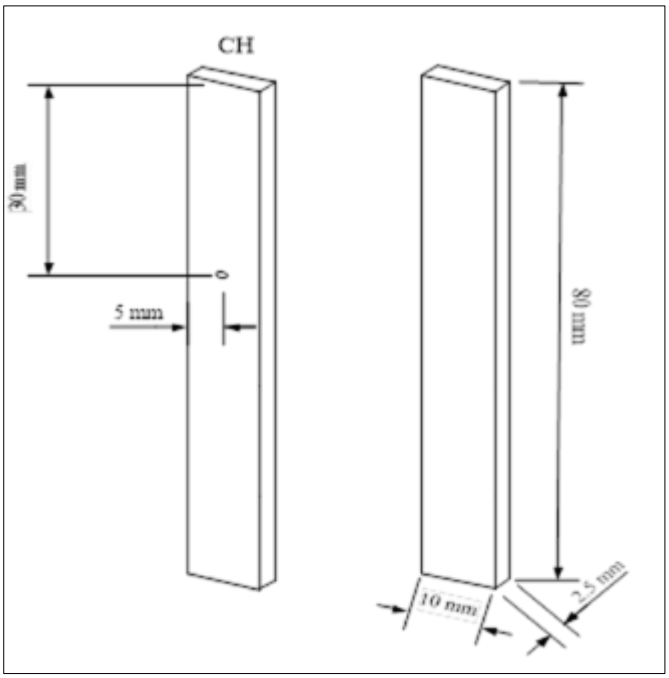


**Figure 4** Types of fatigue model

## 3. Theoretical analyses

The fatigue process begins with the accumulation of damage in a specific area due to repeated loads, which eventually leads to the formation of cracks and their subsequent spread. When one of the cracks grows to a certain extent so that the remaining net portion is not sufficient to bear the applied load, a sudden fracture occurs. In the absence of significant internal defects (large impurities), fatigue cracks usually begin on the surface of the sample and their initial growth is generally in the direction of the greatest strain of sternum. Generally the sites of the beginning of the cracks are either very prior stressful areas such as cracks, craters, scratches or valley-like surface cracks, so by viewing the surface of fatigue fracture we may distinguish three features [13].

- Crack initiation
- Crack Propagation
- Sudden Fracture

### 3.1. The notch and stress concentration

The openings are used for practical purposes and to reduce the weight of the structures for spacecraft or aircraft, that the presence of these openings plays an important role in the design of mechanical structures and the weakening of their behavior, which leads to a redistribution of stresses in the plate that leads to a significant reduction in the stability of the structure, which drew the attention of many researchers in past years. The holes in the engineering designs constitute one of the complex problems facing the designer due to the areas of focus stress local near these openings resulting from the areas of the presence of these holes. These openings become strainer lever areas. The stress concentration is attributed only to the different sections of the shape, the discontinuity of the fixed geometrical shape, and the decrease in the total area [14].

## 4. Numerical analysis

### 4.1. Development of a fatigue model for aluminum alloys.

The general analysis using ANSYS workbench) contains six main steps:

- Define element type.
- Engineering data.
- Geometry.

- Mesh The Model geometry.
- Boundary condition.
- Fatigue solution.

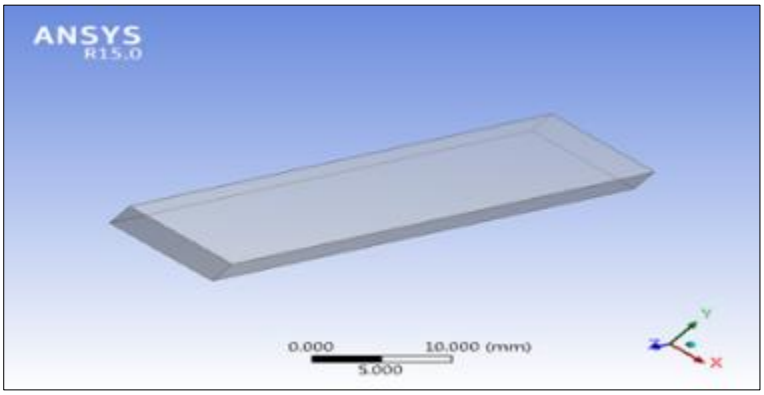


**Figure 5** ANSYS Sample without Notches

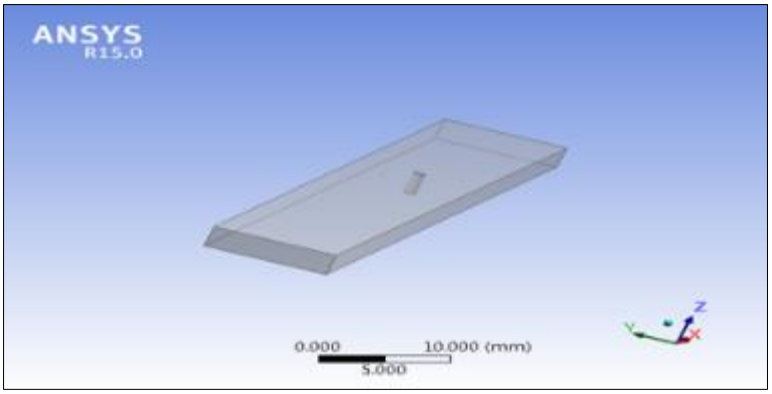


**Figure 6** ANSYS Sample notch analysis

### 4.2. Mesh the model geometry

For this work, the number of elements was (3204) elements with the total number of nodes (17138) knots for the model that does not contain Notch slits) as shown in Figure (7). In the current work, the appropriate size of the grid was 0.9) mm as shown in Table (3). And the number of elements is 3105, with a total number of nodes (16669) knots for contain at notches as shown in figure (8).

**Table 3** Grid independent test (GIT)

| **Mesh size(mm)** | 0.5 | 0.9 | 1.2 | 1.5 | 2 | 3 | 4 | 5 |
|---|---|---|---|---|---|---|---|---|
| **Stress (MPa)** | 81.35 | 80.931 | 79.472 | 79.574 | 78.678 | 83.161 | 84.374 | 84.426 |

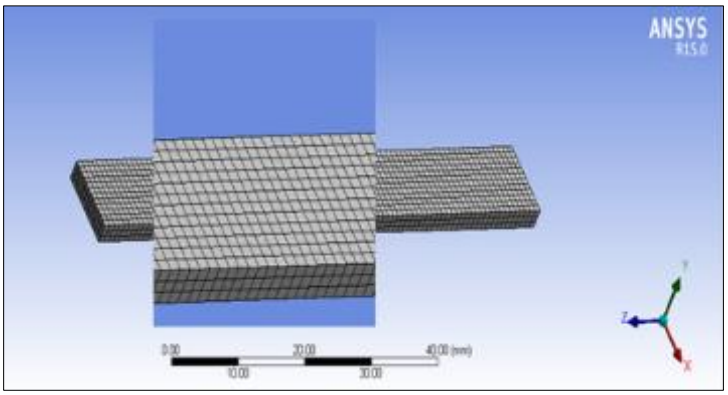


**Figure 7** Mesh (without Notch)

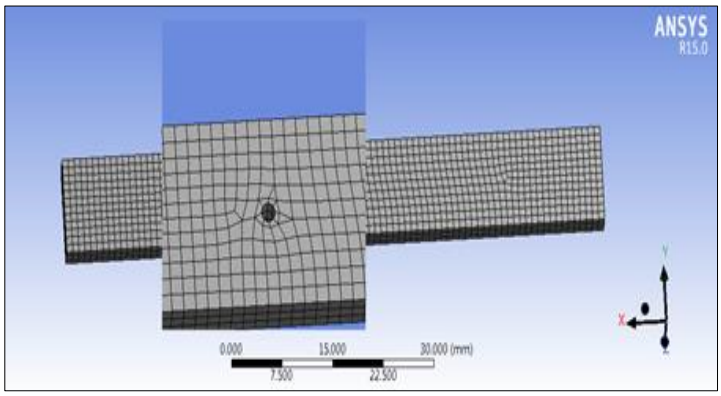


**Figure 8** Mesh (with Notch)

### 4.3. Boundary condition

The next step involved applying appropriate boundary conditions and external loads. The force in ANSYS Workbench will be on one side, and the other side will be fixed support as shown in Figure (9). As for the shape (10), which contains notch, the force is far from the slitting by (50) mm.

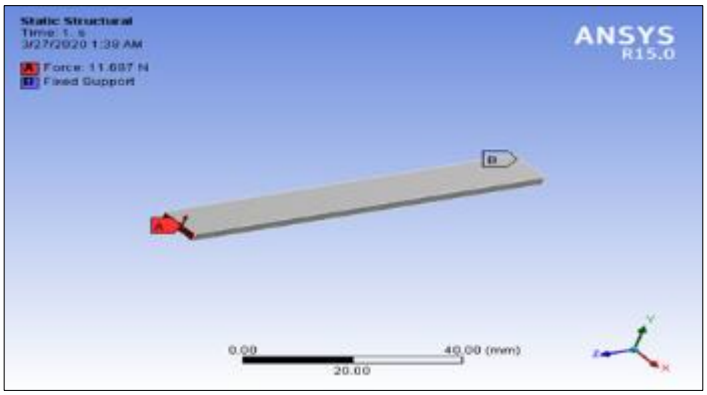


**Figure 9** Fixed support and applying load

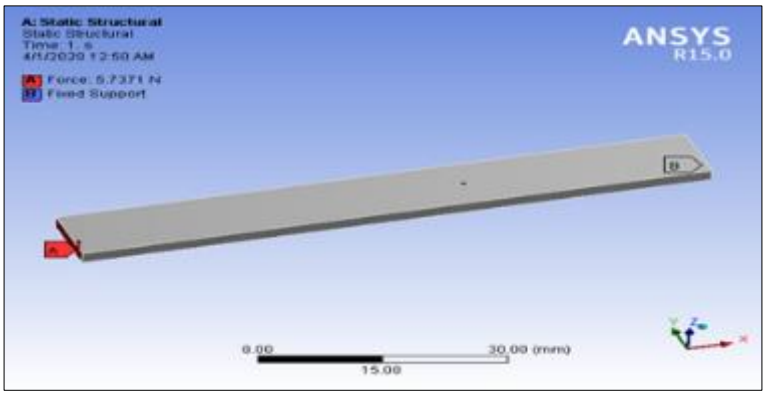


**Figure 10** Fixed support and load with notch

### 4.4. Fatigue Solution

The fatigue results can be obtained from selection fatigue tool and insert life option at different loads in Ansys15.0 workbench.

In order to complete the total solution of any case, other important parameters are added, such as mass density, Poisson ratio, ultimate stress, tensile yield stress and experimental S-N curves, and Young's modulus [15] as shown in the table (4).

**Table 4** Properties Insert to ANSYS (Obtain from Experimental Work

| Type of series | $\sigma_y$ (MPa) | $\sigma_u$ (MPa) | E (GPa) | Poisons Ratio |
|---|---|---|---|---|
| o-2024 | 73.6 | 195.2 | 69 | 0.33 |

## 5. Results and discussion

### 5.1. Fatigue test results (Experimental)

Fatigue test results were performed for two conditions, baseline samples, and median slitting samples. The stress ratio for all tests was R = -1 at a frequency of (60 Hz), and all tests were performed at a rotational speed of 6000 rpm. The practical side is divided as follows.

- Basic Material without Notch.
- Samples containing center Hole.

At this stage, we will study comparing samples with median incision with theoretical and practical samples. The load and stress of the basic samples can be calculated from the following equations mentioned in the device manual.

$$\sigma_b = \frac{6 * L * P}{b * t^3} \quad \ldots\ldots\ldots\ldots (3)$$

As for finding strength and stress in samples that contain a median groove, it is done from the following equations [16].

$$\sigma_{nom} = \frac{6 * M}{(b - d) * t^2} \quad \ldots\ldots\ldots\ldots\ldots \quad (4)$$

$$\sigma_b = K_t * \sigma_{nom} \quad \ldots\ldots\ldots\ldots\ldots\ldots\ldots \quad (5)$$

*5.1.1. Basic Material without Notch*

**Table 5** Stress values, deviation, load, and number of cycles for base samples

| I | Stress (MPa) | $N_f$(EXP) |
|---|---|---|
| 1 | 80 | 2163857 |
| 2 | 100 | 566857 |
| 3 | 123 | 133768 |
| 4 | 138 | 93045 |
| 5 | 161 | 46028 |
| 6 | 169 | 27175 |
| 7 | 177 | 20427 |
| 8 | 207 | 16926 |
| 9 | 230 | 10865 |
| 10 | 246 | 3397 |

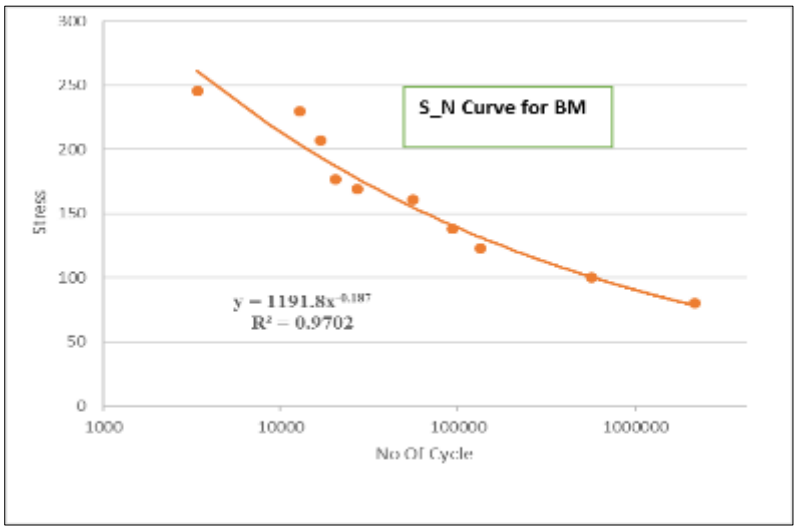


**Figure 11** Curved (S-N) for baseline samples

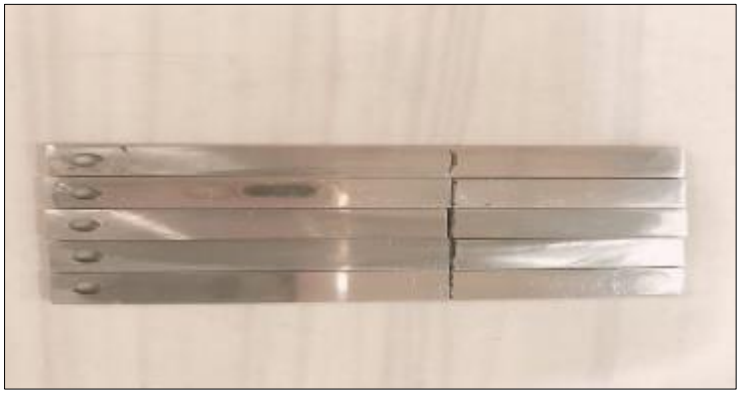

**Figure 12** The location of the fraction in (BM)

*5.1.2. Samples containing center Hole*

**Table 6** Values of Stress, Deviation, Load, and Number of Cycles of Samples (CH)

| I | Stress (MPa) | $N_f$ (EXP) |
|---|---|---|
| 1 | 55 | 1645300 |
| 2 | 71 | 420870 |
| 3 | 85 | 113325 |
| 4 | 96 | 50723 |
| 5 | 112 | 40323 |
| 6 | 117 | 26350 |
| 7 | 123 | 16530 |
| 8 | 144 | 10199 |
| 9 | 160 | 5920 |
| 10 | 171 | 1645 |

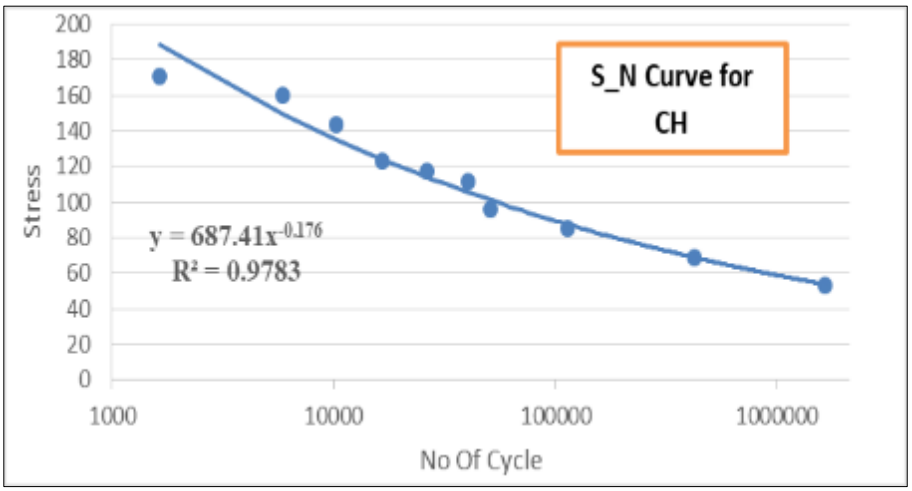


**Figure 13** The S-N curve of notched samples (CH)

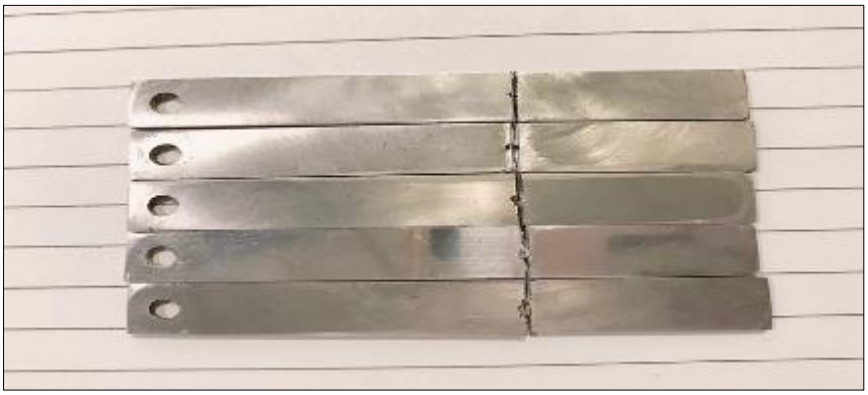

**Figure 14** The location of the fracture in the samples (CH)

### 5.2. Endurance limit and Fatigue Curve (Experimental)

Depending on the shape of the Basquin equation, the fatigue life equations for constant capacitance loads can be represented by blasting with spheres and without them by the following equation

The fatigue curve can be presented by the following equation [17]:

$$\sigma_f = A\,(N_f)^m \qquad \ldots\ldots\ldots\ldots \quad (7)$$

Where: $\sigma_f$ is the applied stress (MPa) at failure?

$N_f$ *:* is the fatigue life (cycles).

*A* and *m:* material constants and may be evaluated by linearizing

Then equation (7) can be written in logarithmic form (15), as follows:

$$\mathrm{Log}\sigma_f = \mathrm{LogA} + m\mathrm{Log}N_f \qquad \ldots\ldots\ldots\ldots \quad (8)$$

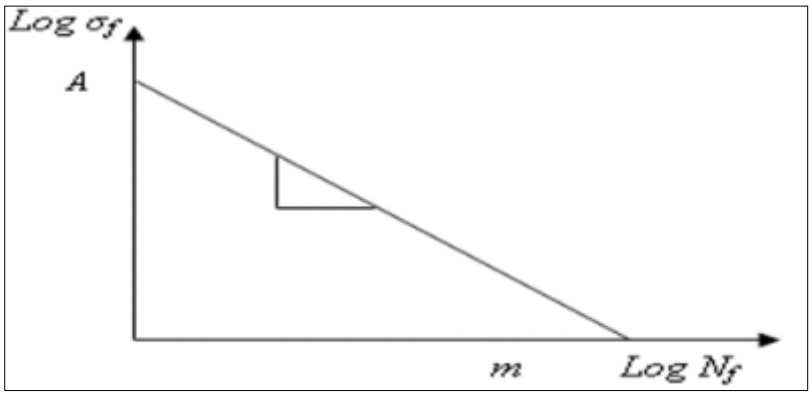


**Figure 15** Is a logarithmic description of the life fatigue equation [15]

From these equations, fatigue strength was extracted after substituting $N_f = (10^6)$in the mentioned equations. Note that streaking reduces fatigue resistance by (35%) from base samples and Table (7) shows the practical fatigue curve equations.

**Table 7** The equations for practical fatigue values

| Material | Curve Equation | Fatigue Limit |
|---|---|---|
| BM | $\sigma_f = 1191.8N_f^{-0.187}$ | 58.5 |
| CH | $\sigma_f = 687.41N_f^{-0.176}$ | 40 |

### 5.3. Numerical Analysis

*5.3.1. Basic samples (BM)*

Figures (16) to (19) show Equivalent Stress, Safety Factor, total deformation and number of cycles for base samples at stress (80 MPa), and other samples were calculated in the same way shown in Table (8).

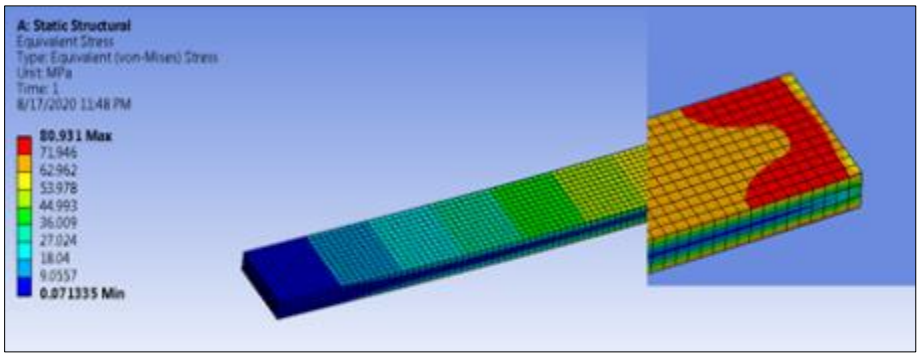


**Figure 16** Von Mises Stress

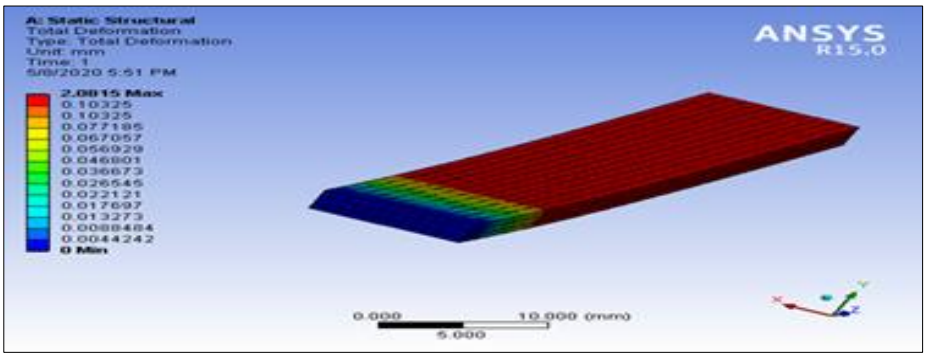


**Figure 17** Total deformation for

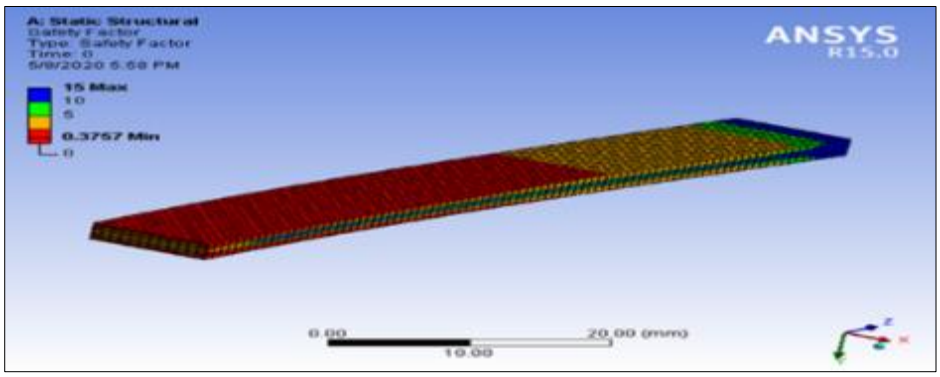


**Figure 18** The Safety Factor

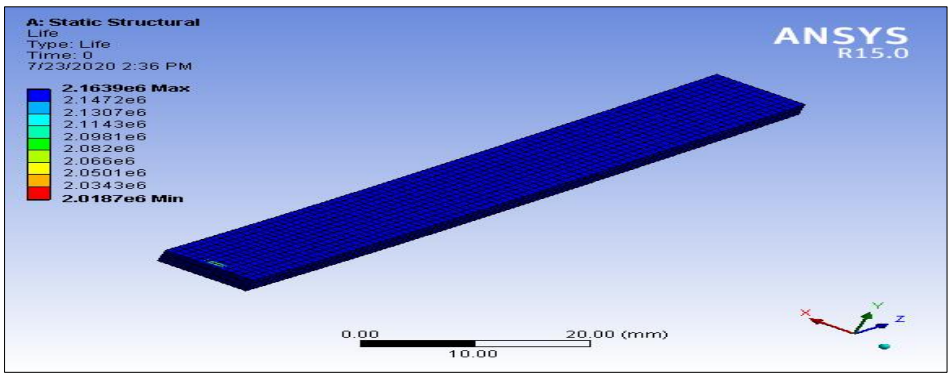


**Figure 19** Available for Fatigue life

**Table 8** The theoretical values through the ANSYS program

| Applied stress (MPa) | Total deformation (mm) | Equivalent stress (MPa) | N. of cycle to failure (NUM) | Safety factor |
|---|---|---|---|---|
| 80 | 0.792 | 81 | 2018700 | 0.986 |
| 100 | 1.020 | 104 | 511050 | 0.766 |
| 123 | 1.239 | 124.6 | 127970 | 0.631 |
| 138 | 1.388 | 140.17 | 88832 | 0.563 |
| 161 | 1.615 | 163.53 | 44124 | 0.484 |
| 169 | 1.685 | 171.32 | 25354 | 0.4641 |
| 177 | 1.784 | 179.11 | 20084 | 0.438 |
| 207 | 2.081 | 210.26 | 16303 | 0.375 |
| 230 | 2.304 | 233.62 | 9984.1 | 0.339 |
| 246 | 2.477 | 249.19 | 0 | 0.315 |

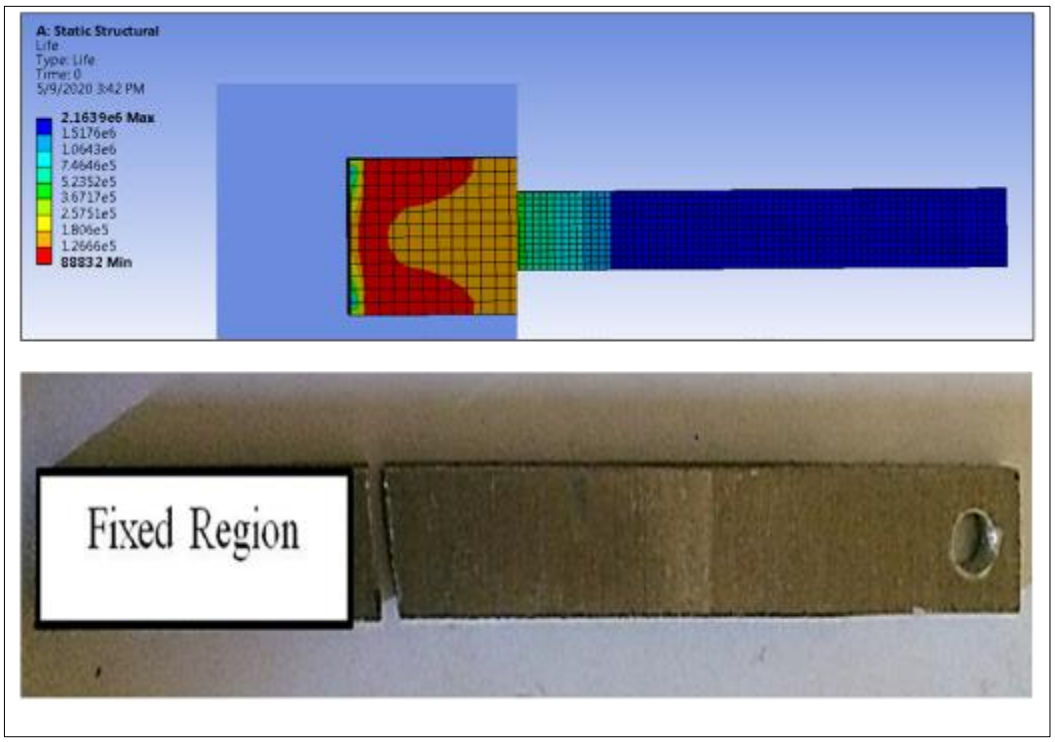


**Figure 20** The location of the fraction for the baseline samples

*5.3.2. Samples containing CH*

Figures (21) to (24) show Equivalent Stress, Safety Factor, total deformation and number of cycles for samples containing a median groove of 1 mm in diameter (171 MPa), and other samples were calculated in the same way and their values are shown in Table (9).

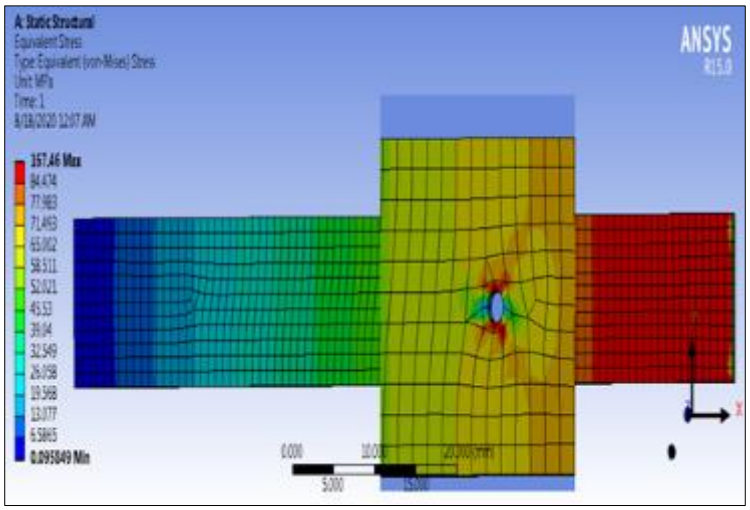


**Figure 21** Equivalent (Von Mises) Stress

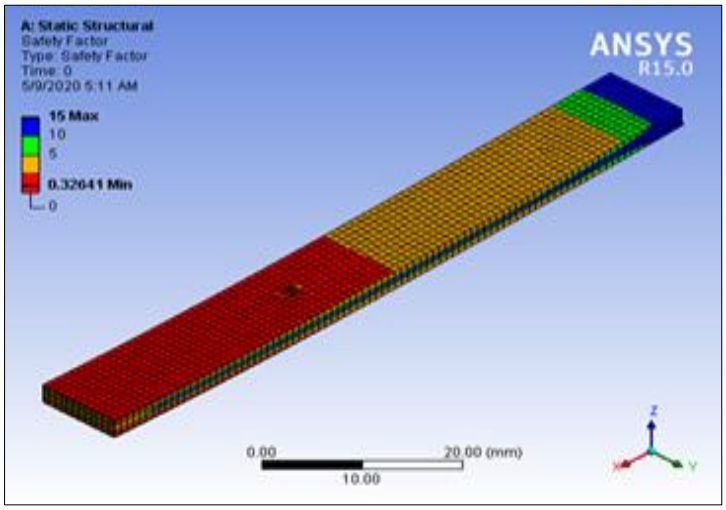


**Figure 22** (Safety Factor)

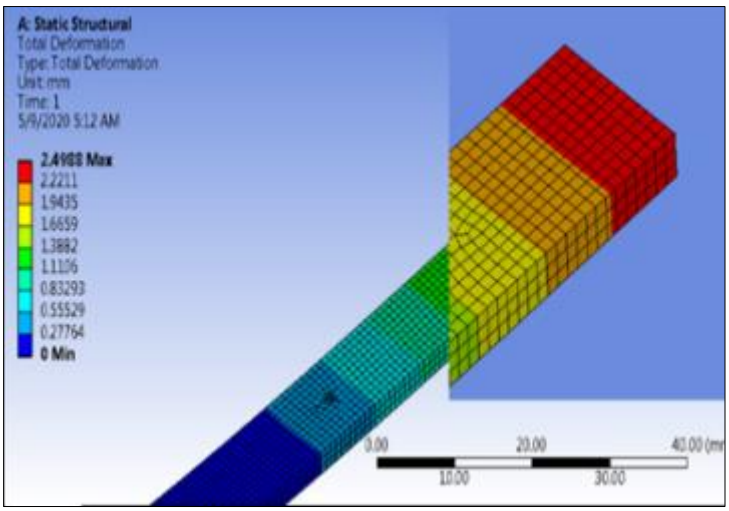


**Figure 23** (Total deformation)

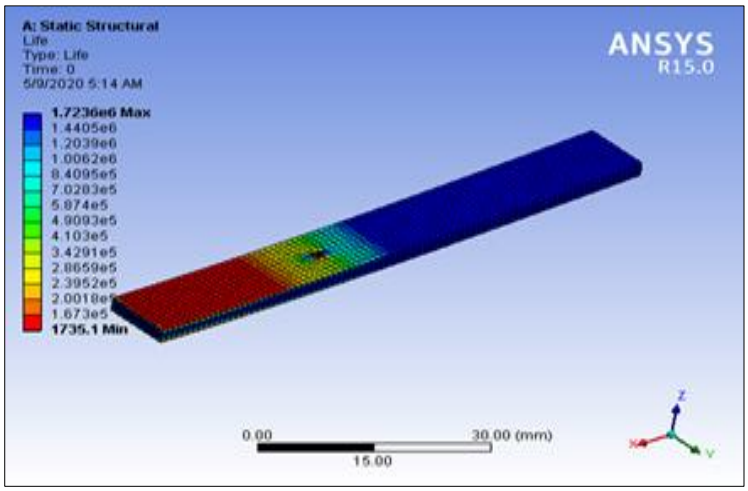


**Figure 24** The (N. of life for)

**Table 9** The theoretical values for samples (CH)

| Applied stress (MPa) | Total deformation (mm) | Equivalent stress (MPa) | N. of cycle to failure (NUM) | Safety factor |
|---|---|---|---|---|
| 55 | 0.795 | 124.31 | 1723600 | 1.025 |
| 71 | 1.024 | 159.68 | 427980 | 0.796 |
| 85 | 1.249 | 191.38 | 114950 | 0.652 |
| 96 | 1.392 | 215.3 | 53891 | 0.585 |
| 112 | 1.606 | 251.19 | 41115 | 0.507 |
| 117 | 1.690 | 263.15 | 28695 | 0.482 |
| 123 | 1.785 | 275.11 | 18274 | 0.456 |
| 144 | 2.088 | 322.95 | 11026 | 0.390 |
| 160 | 2.286 | 358.84 | 6029.4 | 0.356 |
| 171 | 2.498 | 382.76 | 1735.1 | 0.326 |

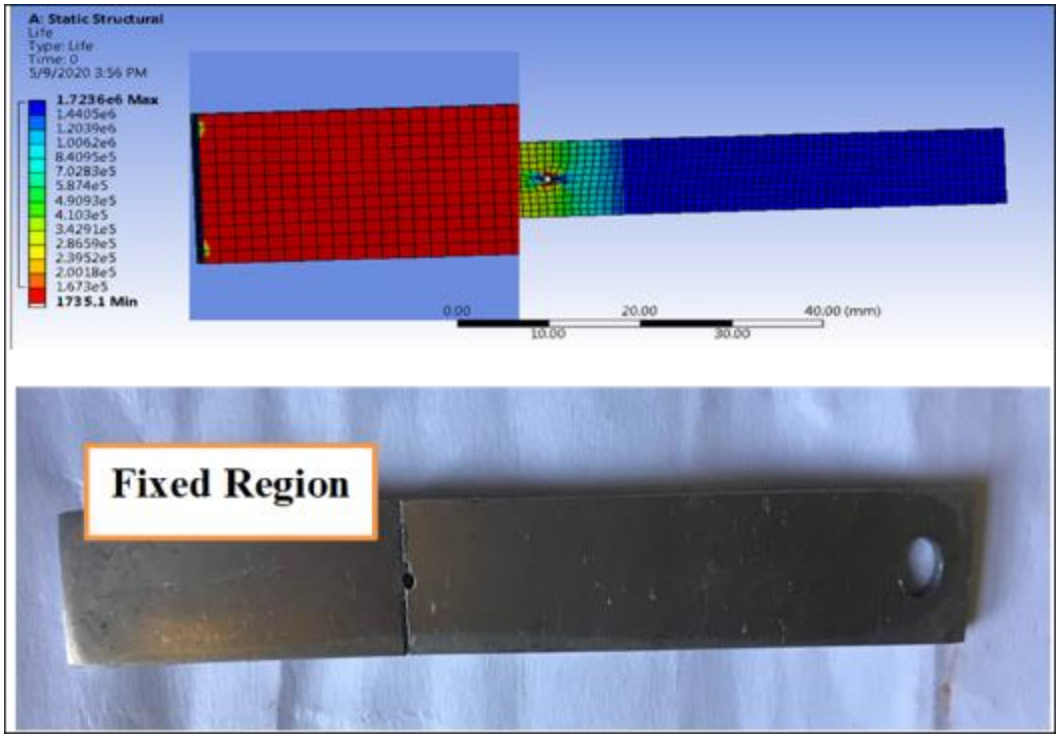


**Figure 25** The fractional location between Experimental and theoretical for CH

### 5.4. Endurance limit and Fatigue Curve (NUM)

Thus reducing the number of cycles and reducing fatigue resistance by (34.86%) from the base samples. The fatigue curve equations are shown in Table (10).

**Table 10** The equations for the fatigue curve (theoretical)

| Material | Curve Equation (NUM) | Fatigue Limit |
|---|---|---|
| BM | $\sigma_f = 1190.2N^{-0.185}$ | 60.34 |
| CH | $\sigma_f = 662.16N^{-0.175}$ | 39.4 |

## 6. The comparison between Experimental and theoretical.

The results showed that the compatibility is good between theoretical and practical, but there is a slight difference in the number of calculated cycles between practical and theoretical, which is less than 10% and is acceptable, and the reason is due to the discrepancy between practical and theoretical values due to the state of the process, which cannot be controlled and also was not accurate due to the equipment and the environment.

**Table 11** The difference between theoretical and Experimental samples (BM)

| **Stress (MPa)** | $N_f$ $(EXP)$ | $N_f$ $(NUM)$ | **Error%** |
|---|---|---|---|
| 80 | 2163857 | 2010400 | 7 |
| 100 | 566857 | 511050 | 9.84 |
| 123 | 133768 | 127970 | 4.33 |
| 138 | 93045 | 88832 | 4.52 |
| 161 | 46028 | 44124 | 4.13 |
| 169 | 27175 | 25354 | 6.7 |
| 177 | 20427 | 20084 | 1.68 |
| 207 | 16926 | 16303 | 3.68 |
| 230 | 10865 | 9984.1 | 8.1 |
| 246 | 3397 | 0 | 1 |

**Table 12** The difference between theoretical and Experimental samples (CH)

| **Stress (MPa)** | $N_f$ $(EXP)$ | $N_f$ $(NUM)$ | **Error%** |
|---|---|---|---|
| 55 | 1645300 | 1723600 | 4.54 |
| 71 | 420870 | 427980 | 1.66 |
| 85 | 113325 | 114950 | 1.41 |
| 96 | 50723 | 53891 | 5.87 |
| 112 | 40323 | 41115 | 1.92 |
| 117 | 26350 | 28695 | 8.17 |
| 123 | 16530 | 18274 | 9.54 |
| 144 | 10199 | 11026 | 7.5 |
| 160 | 5920 | 6029.4 | 1.81 |
| 171 | 1645 | 1735.1 | 5.19 |

*Nomenclature*

| **Symbols** | |
|---|---|
| $F$ | Force, N |
| σ | Stress, MPa |
| A | Area, $m^2$ |
| ε | Strain, |
| L | Length, mm |
| E | Modulus of elasticity, GPa |
| P | The Load, N |
| b | Width, mm |
| T | thickness, mm |
| Δ | deflection, mm |

| | |
|---|---|
| $\sigma_b$ | Stress bending, MPa |
| M | Moment of inertia, N.mm |
| D | Diameter of Hole, mm |

## 7. Conclusion

- The more stress on the samples, the less the number of cycles, and consequently, the sample will be broken and failure will occur.
- Grooving in the samples works to focus the stress and thus increase the stress value that causes the failure process faster than the base samples.
- Through the equations we note that the grooves reduce the fatigue resistance by (35%) of the base samples in the practical part, while in the theoretical part we notice that the grooves reduce the fatigue resistance by (34.86%) of the core samples.

## Compliance with ethical standards

*Acknowledgments*

The authors would like to thank the Department of Mechanical Engineering at Tikrit University which has supported and guided this research.

*Disclosure of conflict of interest*

There is no conflict of interest.

## References

[1] Emad Touma Bani Karsh (2014). A study of the effect of changing the stress ratio on the onset of fatigue cracking of the first phase. Al-Qadisiyah Journal of Engineering Sciences, 7 (4), a187-200.

[2] Hazem Khalil Khalaf, (2000). Behavior of short and long fatigue cracks in medium carbon steel. PhD dissertation, University of Technology.

[3] Alalkawi, H. J., & Shaker, M. S. (1993). Mechanical Properties Improvement of Duraluminium 2024-T4 under Heat Chemical Treatment. Journal of M.T.C, P.111 – 118.

[4] Jamal Muhammad Hamad, (2010). Studying the corrosion phenomenon of aluminum alloy 2024 and the effect of this phenomenon on the mechanical properties and crystalline structure of the alloy. PhD thesis, Damascus University.

[5] Ahmed Saadi Mohamed, (2003). Estimation of the fatigue life of an aircraft fuselage under the influence of different flight loads. Master's thesis, University of Technology.

[6] Bader, Q., & Kadum, E. (2014). Effect of V notch shape on fatigue life in steel beam made of AISI 1037. International Journal of Engineering Research and Applications, 4(6), 39-46.

[7] Drake, D. W. (1946). The Effect of Notches on Static and Fatigue Strength. Journal of the Aeronautical Sciences, 13(5), 259-269. doi:10.2514/8.11366.

[8] Shaima Abdul Khader Hamza (2018). Effect of constant and variable amplitude loads on the fatigue life of low carbon alloy steel /Effect of Fixed and Variable Amplitude Loads on the Fatigue Life of Low Carbon Steel Alloy. Journal of University of Babylon for Pure and Applied Sciences, 26(1), 221-227.

[9] Martínez, J. M. G., Adriano, V. S. R., Araújo, J. A., Ferreira, J. L. A., & da Silva, C. R. M. (2019). Geometrical size effect in the fatigue life predictions of aluminum wires with micro holes using methods of the critical distance. Engineering Fracture Mechanics, 209, 147-161. doi:10.1016/j.engfracmech.2018.12.034

[10] Bray, J. (1990). Properties and selection: Nonferrous alloys and special purpose materials. ASM Metals handbook, 92.

[11] Mott, R. L., & Tang, J. (2004). Machine elements in mechanical design (Vol. 4): Pearson Prentice Hall Upper Saddle River.

[12] Standard, A. (2001). E3, Standard guide for preparation of metallographic specimens. West Conshohecken, PA: ASTM International.

[13] Ellyin, F. (2012). Fatigue damage, crack growth and life prediction: Springer Science & Business Media.

[14] Ahmed Hadi Abboud (2015). Study of the elastic-elastic behavior of a stretched plate with two circular holes. Babylon University Journal, 23(4), 759-772..

[15] Jawad, A., A. (2014). Fatigue Behavior and Mechanical Properties of Similar and Dissimilar Friction Stir Welded of Aluminum Sheets. M.Sc. Thesis, Department of Machinal Engineering and Equipment, University of Technology.

[16] Pilkey Peterson's, W., D. (2000). Stress Concentration Factors. 2nd edition, John Wileys and Sons Inc, 508 pp. (Chart 4.83 p. 359 § 4.6.4 p. 240).

[17] Majeed, M. H. (2009). Accumulated damage in fatigue-creep interaction of aluminum alloy 2024-T4 blade material. PhD thesis, University of Technology.